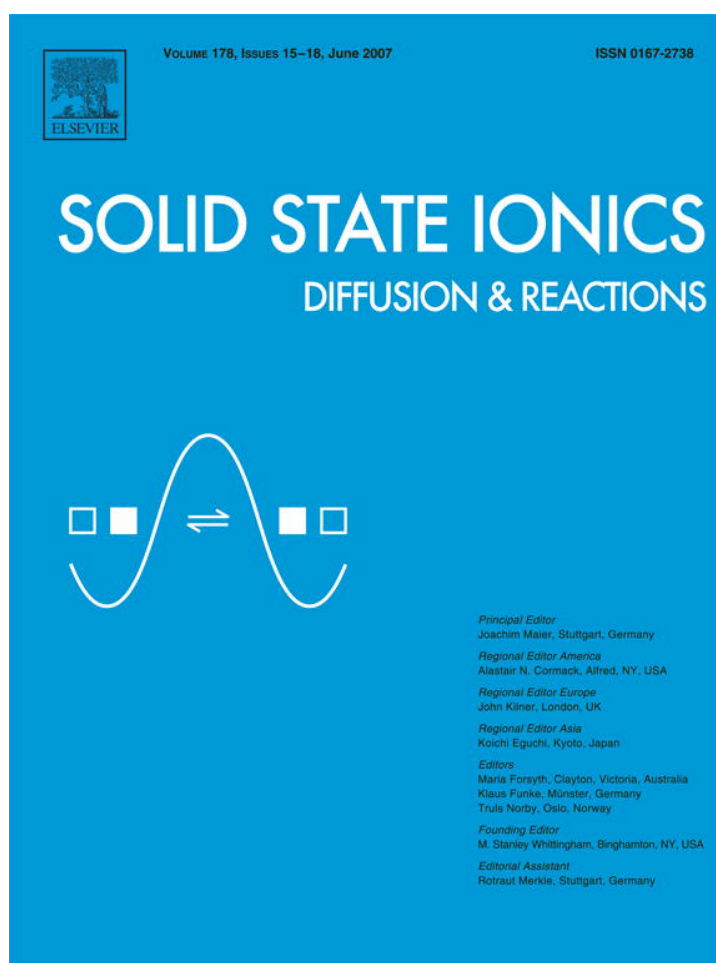


Provided for non-commercial research and educational use only.
Not for reproduction or distribution or commercial use.



This article was published in an Elsevier journal. The attached copy is furnished to the author for non-commercial research and education use, including for instruction at the author's institution, sharing with colleagues and providing to institution administration.

Other uses, including reproduction and distribution, or selling or licensing copies, or posting to personal, institutional or third party websites are prohibited.

In most cases authors are permitted to post their version of the article (e.g. in Word or Tex form) to their personal website or institutional repository. Authors requiring further information regarding Elsevier's archiving and manuscript policies are encouraged to visit:

<http://www.elsevier.com/copyright>

Intrinsically proton conducting polymers and copolymers containing benzimidazole moieties: Glass transition effects

Richard C. Woudenberg^a, Ozgur Yavuzcetin^b, Mark T. Tuominen^b, E. Bryan Coughlin^{a,*}

^a Department of Polymer Science and Engineering, University of Massachusetts at Amherst, 120 Governors Drive, Amherst, MA 01003, United States

^b Department of Physics, University of Massachusetts at Amherst, 411 Hasbrouck Laboratory, Amherst, MA 01003, United States

Received 5 October 2006; received in revised form 28 March 2007; accepted 9 May 2007

Abstract

Proton conducting polymers and copolymers containing tethered benzimidazole moieties spanning a wide range of glass transition temperatures (2–113 °C) have been prepared. Conductivity versus temperature plots of the homopolymers display the competing effects of mobility and charge carrier density. Consistent with literature reports, T_g values of benzimidazole-containing polymers increased over the parent polymer, however, successful reduction of T_g was accomplished by copolymerizing a benzimidazole functional acrylate monomer (B5A) with poly(ethylene glycol) methyl ether acrylate (PEGMEA). The reduction in T_g is thought to occur through disruption of intermolecular forces between benzimidazole units. Evaluation of conductivity as a function of temperature by ac impedance methods indicate that decreasing T_g through copolymerization results in conductivity increases over the low and intermediate temperature range (40–160 °C). Copolymer T_g decreases with increasing PEGMEA content, and conductivity at 40 °C can be increased by nearly 2.5 orders of magnitude over B5A homopolymer. However, conductivity at high temperatures (>160 °C) decreases due to charge carrier dilution by the addition of PEGMEA.

© 2007 Elsevier B.V. All rights reserved.

Keywords: Anhydrous proton conduction; Benzimidazole; Fuel cell membrane; Proton exchange

1. Introduction

As the supply of fossil fuels steadily declines, new efficient sources of renewable energy must be identified to keep up with the world's increasing power demands. Hydroelectric, solar, wind, and geothermal are all sources of stationary renewable power that are currently being utilized to various degrees. However, as the global community becomes increasingly mobile, there is a need for clean portable power sources to sustain current standards of living [1–3]. Polymer electrolyte membrane fuel cells (PEMFCs) operate at relatively low temperatures with high efficiency and power density and little or no hazardous emissions [2,3], making them an attractive power source for vehicular transport and portable electronic devices [4]. However, several remaining challenges must be overcome before PEMFCs become viable power sources, including generation of more cost effective materials that

offer improved performance over present technology [4–6]. While improvements are necessary in all components of PEMFCs, a significant area of exploration is the development of new polymer electrolyte membranes with improved durability and performance. Thus far, major research efforts have focused on membranes that rely on water as the media for proton transport [5–7], however, the maximum use temperature of these membranes is intrinsically limited to approximately the boiling point of water.

An attractive alternative approach, using amphoteric nitrogen containing heterocycles as the proton conducting species has been proposed by Kreuer [8,9]. The proton conductivity of membranes using heterocyclic motifs, either as dopants or as pendant groups, in polymer membranes does not depend on relative humidity and could thus enable the use of PEMFCs without the need of external humidification and at temperatures well above 100 °C. The increase in the operation temperature will increase the efficiency of the fuel cell and reduce the overall cost by decreasing the required platinum catalyst loading in the membrane electrode assemblies and simplifying the overall heat

* Corresponding author. Tel.: +1 413 577 1616; fax: +1 413 545 0082.

E-mail address: Coughlin@mail.pse.umass.edu (E.B. Coughlin).

management of the system [10]. Further studies using imidazole and benzimidazole as the proton conducting groups have revealed that their proton conductivity depends on the local mobility of the heterocycles in the polymer films and the effective concentration of mobile protons within the membranes [11–14].

Investigation into the local mobility of polymer tethered benzimidazole by Persson and Jannasch [15] indicate that the effect is much more pronounced at low to moderate temperatures, while heterocycle concentration plays a dominant role at higher temperatures. However, these two effects are at odds; while increasing the mol% of benzimidazole units results in increased high temperature conductivity, there is a subsequent increase in polymer T_g , resulting in dramatically decreased conductivity at low temperatures. Although target operating temperatures of future generation PEMFCs is greater than 100 °C, the membrane must have high enough conductivity at low temperatures for initial start-up, therefore, further investigation into T_g effects on proton conduction is necessary. In this article we report several polymers and copolymers containing tethered benzimidazole moieties to explore the effect of polymer glass transition temperature on conductivity over a wide temperature range.

2. Experimental

2.1. Materials

2,2,2-Trichloroethylchloroformate, Acryloyl chloride, Methacryloyl chloride, 5-Norbornene-2-carboxylic acid, Dicyclohexylcarbodiimide, Dimethylaminopyridine, and Grubbs second generation catalyst were received from Aldrich Chemical and used without further purification. Poly(ethylene glycol) methyl ether acrylate (M_n , 454 g/mol) was received from Aldrich Chemical and passed through basic alumina to remove added inhibitors prior to polymerization. 2,2'-Azobis(2-methylpropionitrile) was received from Aldrich Chemical and recrystallized from methanol prior to use. Triethylamine was received from Aldrich chemical and dried over molecular sieves. Solvents were received from VWR International and used without further purification. The *N*-troc hydroxypentylbenzimidazole, **1**, was prepared as previously reported [16].

2.2. Instrumentation

^1H (300 MHz) and ^{13}C NMR (75 MHz) spectra were obtained on a Bruker DPX-300 NMR Spectrometer. Gel permeation chromatography (GPC) was performed with a Polymer Lab LC 1120 high-performance liquid chromatography pump equipped with a Waters differential refractometer detector. The mobile phase was dimethylformamide with a flow rate of 1.0 mL/min. Molecular weights were calculated vs. narrow molecular weight poly(methyl methacrylate) standards. Electrochemical impedance data was obtained using a Solartron 1287 potentiostat/1252A frequency response analyzer in the 0.1 Hz–300 kHz range. Glass transition temperatures were obtained by differential scanning calorimetry (DSC) using a TA

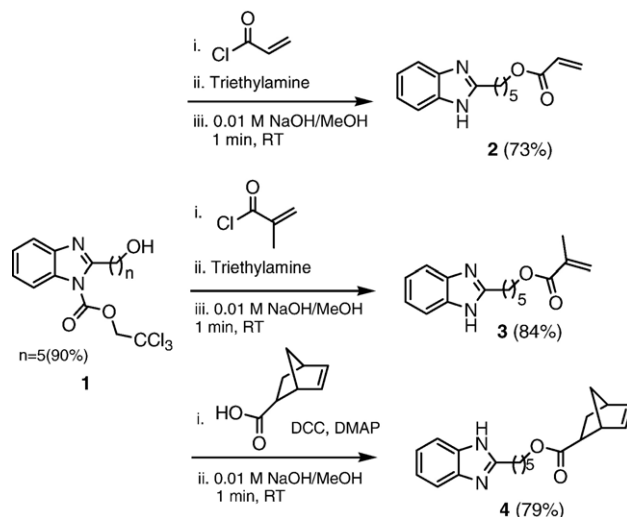
Instruments Dupont DSC 2910 at a heating rate of 10 °C/min from under a flow of nitrogen (50 mL/min). Thermogravimetric analysis (TGA) was performed using a Perkin Elmer Pyris 1 TGA with nitrogen flow of 20 mL/min. Fourier transform IR (FTIR) spectra were obtained with a Bruker IFS 66v/S, samples were prepared in a diamond ATR and scans performed under vacuum.

2.3. Monomer synthesis

Three benzimidazole functional monomers were prepared from *N*-troc hydroxypentylbenzimidazole (**1**) [16], resulting in monomers with consistent tether length between the polymerizable group and the benzimidazole, Scheme 1. The benzimidazole functional acrylate (**2**) and methacrylate (**3**) were prepared by reaction of **1** with acryloyl chloride and methacryloyl chloride respectively, followed by *N*-troc deprotection in basic methanol. The norbornene derivative was prepared by coupling 5-norbornene-2-carboxylic acid with **1** via DCC/DMAP followed by troc deprotection in basic methanol to give **4**. The monomers prepared have the benzimidazole moieties attached via an ester linkage. We recognize that this presents concerns for the implementation of these polymers in actual fuel cell membranes, however, the chemistry was chosen for synthetic ease to probe structure–conductivity relationships.

2.4. Polymerization

Free radical polymerization of **2** and **3** using AIBN as the initiator were performed in septum capped scintillation vials under nitrogen at 70 °C in benzene for 10–30 min. The resulting viscous solutions were diluted with DMF and the polymer precipitated in excess ethyl acetate, giving the polymers B5A and B5MA in good yield (79% and 81% respectively). Molecular weight data determined by GPC (DMF/0.01 M LiCl mobile phase) was obtained for both polymers with B5A giving a M_n of 328,000 g/mol ($M_w/M_n=2.44$) and B5MA giving a M_n of 184,000 g/mol ($M_w/M_n=2.37$).



Scheme 1. Synthesis of benzimidazole functional monomers.

Table 1
Polymer physical properties

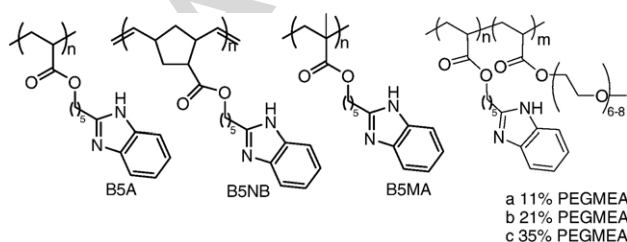
Polymer	% Yield	T_g , °C	Decomp. onset, °C	M_n	M_w/M_n	PEGMEA (mol%)
B5MA	81	113	280	184,000	2.37	0
B5NB	89	98	295	107,000	1.57	0
B5A	79	88	225	328,000	2.44	0
B5A-PEGMEA 11	54	62	270	N/A	N/A	11
B5A-PEGMEA 21	65	43	270	N/A	N/A	21
B5A-PEGMEA 35	58	2	270	N/A	N/A	35

Free radical random copolymerizations of **2** and poly(ethylene glycol) methyl ether acrylate (PEGMEA) with AIBN were performed in septum capped scintillation vials under nitrogen at 60 °C in benzene for 30 min. The resulting viscous solutions were diluted with DMF and the polymer precipitated in excess ethyl acetate to remove residual **2** and AIBN. A second precipitation from DMF into water was required to remove residual PEGMEA, therefore, only moderate yields were obtained (Table 1). Molecular weight data was not obtainable by GPC due to polymer interaction with the stationary phase. Copolymers were prepared with 10, 20, and 30 mol% PEGMEA in the feed. Comonomer incorporation was determined by ^1H NMR by calculating the ratio of aromatic protons on the benzimidazole unit to the methyl protons of the methyl ether, providing the values calculated in Table 1.

Polymerization of **4** was accomplished by ROMP performed in dichloromethane using Grubbs 2 catalyst at 100:1 monomer to catalyst ratio, affording the polymer B5NB in good yield (89 %). Molecular weight determination by GPC indicated an M_n of 107,000 g/mol and $M_w/M_n=1.57$. Free standing films of all polymers and copolymers were prepared according to the procedure outlined in Section 2.6.

2.5. Polymer characterization

The polymers were confirmed to be solvent free as determined by ^1H NMR. Glass transition temperatures for the polymers and copolymers (Scheme 2) were obtained by differential scanning calorimetry (DSC). Samples were cycled at a ramp rate of 10 °C/min between -40 °C and 180 °C, the first cycle was used to erase thermal history and the second cycle was used to determine T_g values from the heating curves values are reported in Table 1. Decomposition temperatures of all polymers and copolymers were determined by thermogravimetric analysis (TGA). Samples were heated at a ramp rate of 10 °C/min from



Scheme 2. Benzimidazole containing homopolymer and B5A-PEGMEA copolymer structures.

25 °C to 600 °C under a nitrogen atmosphere, onset of decomposition is reported as the temperature corresponding to 5% weight loss (Table 1). Polymer B5A displayed a lower decomposition temperature than either B5MA or B5NB, therefore to assure material stability during conductivity testing B5A was heated at a ramp rate of 2 °C/min from 40 °C to 200 °C, held at 200 °C for 5 min, then cooled back to 40 °C at a ramp rate of 2 °C/min (all under a nitrogen atmosphere) estimating the time spent at each temperature during conductivity vs. temperature measurements. After an initial loss of absorbed water, mass loss was ~4 wt.%. To assure that degradation did not occur during the temperature sweep an FTIR trace of the resulting polymer was obtained. A comparison to a B5A control FTIR is displayed in Fig. 1 where it can be seen that no chemical changes occurred during the thermal cycle.

2.6. Membrane preparation

Membranes of B5A, B5NB, B5MA and B5A-PEGMEA 11 and 21 for ac impedance measurements were prepared by casting solutions of each polymer onto a glass plate. Removal of solvent was accomplished by drying in vacuo at room temperature for 18 h, followed by soaking in methanol (3 × 3 min) and air drying. The resulting films were submerged in water and removed from the glass after 3–4 h, then dried in vacuo at room temperature for 18 h. Membranes of B5A, B5NB, B5MA, and B5A-PEGMEA 11 were dried in vacuo for an additional 24 h at 60 °C, whereas B5A-PEGMEA 21 was dried in vacuo an additional 48 h at room temperature (due to the low T_g) to assure removal of residual water. Membranes of B5A-PEGMEA 35 prepared in a similar manner were not processable, the low T_g made removal of the membrane from the glass exceedingly difficult. Therefore, a film of B5A-PEGMEA 35 was cast directly onto a blocking electrode followed by drying in vacuo at room temperature for 18 h then at 60 °C for 48 h. Polymers B5A, B5NB, B5MA and B5A-PEGMEA 11 were cast from DMF while B5A-PEGMEA 21 and B5A-PEGMEA 35 were cast from a DMF/DMSO blend (1/1).

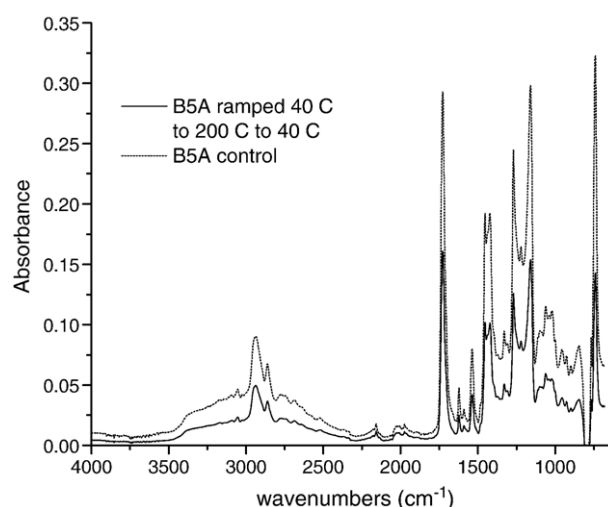


Fig. 1. FTIR traces of B5A and B5A thermally cycled between 40 °C and 200 °C.

2.7. Conductivity measurements

The ac impedance measurements were performed under vacuum to assure an anhydrous environment. Free-standing membranes were clamped between two blocking electrodes followed by application of 100 mV at alternating current from 3×10^5 Hz to 1×10^{-1} Hz. Resistance values were taken at the minimum imaginary response in a Z' vs. Z'' plot to determine conductivity in the dc limit.

3. Results and discussion

Three polymer backbones were chosen to produce a range of T_g 's, poly(acrylate) materials for a low T_g (cf. poly(ethylacrylate) $T_g = -25$ °C [17]), unsaturated polynorbornene by ring-opening metathesis polymerization (ROMP) for an intermediate T_g , ~ 40 °C [18], and poly(methylacrylate) materials (cf. poly(ethyl methacrylate) $T_g \sim 65$ °C [17]) for a high T_g . Local mobility and heterocycle reorientation are affected by the tether length and flexibility [19], therefore, the tether length was kept consistent to eliminate tether length as a conductivity variable. Monomers were prepared containing benzimidazole moieties attached by a five carbon tether to the respective functional group, resulting in polymers with T_g values ranging from 88 °C to 113 °C (Table 1). Increases in T_g over expected values are most likely due to decreased mobility induced by aggregation, hydrogen bonding, and π - π interactions of the benzimidazole side chains. The molecular interactions between tethered benzimidazole strongly affects polymer T_g . Polysiloxane materials with 60 mol% tethered benzimidazole show a T_g of 57 °C, an increase of nearly 180 °C over the parent polymer [15].

3.1. Homopolymer conductivity

The conductivity in polymeric systems depends on the charge carrier density and the mobility of the system, such that changes in either variable influences proton transport. Conduc-

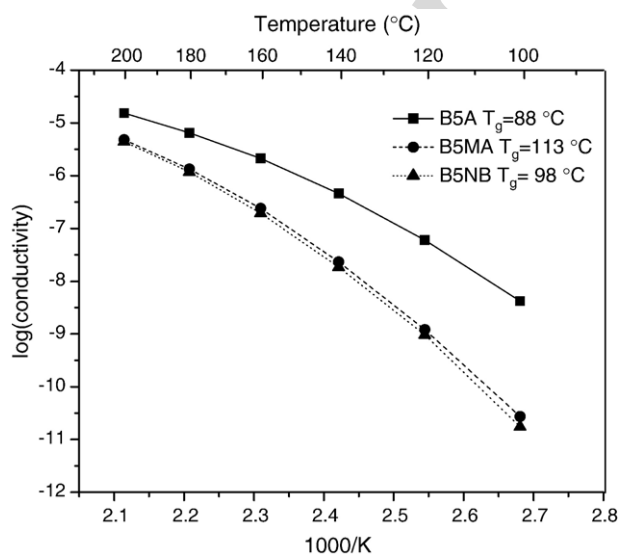


Fig. 2. Conductivity vs. temperature for benzimidazole homopolymers.

Table 2

Benzimidazole content and conductivity data

Polymer	wt.% of Bimi	Conductivity at 40 °C (mS/cm)	Conductivity at 120 °C (mS/cm)	Conductivity at 200 °C (mS/cm)
B5MA	43	N/A	5.50E-07	0.0048
B5NB	36	N/A	1.80E-06	0.0024
B5A	46	4.80E-09	2.20E-05	0.015
B5A-PEGMEA 11	37	4.50E-09	1.40E-05	0.0092
B5A-PEGMEA 21	31	5.70E-08	6.70E-04	0.0064
B5A-PEGMEA 35	23	3.00E-06	7.50E-04	0.011

tivity values of B5A, B5NB, and B5MA from 100 °C to 200 °C are displayed in Fig. 2 with corresponding T_g values, wt.% benzimidazole (Bimi) content is listed in Table 2. By comparing conductivity as a function of T_g , B5A ($T_g = 88$ °C) displays the highest conductivity over the entire temperature range due to increased chain mobility over B5NB ($T_g = 98$ °C) and B5MA ($T_g = 113$ °C). This mobility allows the protonic charge carriers greater range of motion, thus lowering the barrier for heterocyclic rearrangement, facilitating proton diffusion through the material [20,21]. However, the nearly identical conductivity curves observed for B5NB and B5MA indicates that the effect of charge carrier density and mobility are in strong competition. A normalized plot of conductivity as a function of T_g is shown in Fig. 3, where the two effects can be better observed. Conductivity in polyelectrolytes as a function of temperature does not follow Arrhenius behavior, but can be fitted to a Vogel–Tamman–Fulcher (VTF) equation [22].

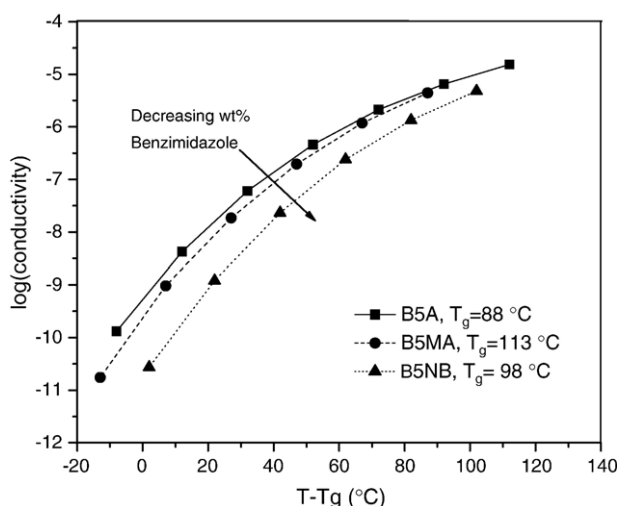
$$\sigma = \sigma_0 \exp[-B/(T - T_0)]$$

The conductivity as a function of temperature depends on the reference temperature, T_0 , a temperature somewhat below T_g in polymeric systems. Since the conductivity is in part governed by the free volume conformational changes [13] it is expected that $\log(\sigma)$ vs. $T - T_g$ curves would converge given a constant protonic charge carrier density. As can be seen in Fig. 3 the curves do not converge, but show a downward trend with decreasing benzimidazole content.

The acrylate polymer B5A showed conductivity of 0.015 mS/cm at 200 °C, nearly an order of magnitude larger than both B5NB and B5MA (0.0024 mS/cm and 0.0048 mS/cm respectively). There is a positive effect on conductivity by increasing mobility as seen by comparing B5A and B5MA, however, the competing effect of charge carrier density reduction is clearly seen by comparing B5NB and B5MA. The two competing effects can be investigated by effecting further reduction in T_g through copolymerization of B5A with a low T_g comonomer.

3.2. Copolymer conductivity

To disrupt the benzimidazole interactions and reduce the T_g , 2 was copolymerized with poly(ethylene glycol) methyl ether acrylate (PEGMEA, $T_g \sim -55$ [23]). Two recent reports by Persson and Jannasch [24,25] investigate the use of PEG as a

Fig. 3. Conductivity vs. $T-T_g$ for benzimidazole homopolymers.

way of reducing T_g in polymers with tethered benzimidazole units. The first attaches benzimidazole heterocycles to polystyrene via ethylene glycol tethers, resulting in the increase of the T_g of the parent polymer of approximately 100 °C. In this case, a benzimidazole is attached to every ethylene glycol repeat unit, giving a high density of heterocycles and the observed T_g increase. The second utilizes PEG block copolymers to introduce varying fractions of tethered benzimidazole, resulting in effective T_g reduction as the mole fraction of benzimidazole is decreased. In our case, as the mole fraction of PEG is increased the benzimidazole mole fraction is decreased through random incorporation of PEG side chains. The net result being that T_g is reduced (Table 1), resulting in increased conductivity values at lower temperatures even though the charge carrier density is reduced, potentially expanding the useful temperature range of anhydrous proton conducting materials.

Conductivity as a function of temperature from 40 °C to 200 °C for the B5A-PEGMEA copolymers is displayed in Fig. 4, B5A homopolymer data is shown for comparison. Three temperature regimes are defined, low (<80 °C), intermediate (80–160 °C) and high (>160 °C). With the exception of B5A-PEGMEA 11, conductivity increases in the low temperature regime while the values converge at high temperatures to a point about 0.5 orders of magnitude lower than B5A homopolymer. The decrease is indicative of the reduction in charge carrier density as benzimidazole is replaced by PEG in the copolymers. Representative data points for each temperature regime are shown in Table 2, of particular interest is B5A-PEGMEA 35 copolymer which displays the most pronounced effect in the low temperature regime, where conductivity increases over B5A homopolymer are 2–3 orders of magnitude. Additionally, moderate improvements are maintained in the intermediate temperature regime (1–2 orders of magnitude) with only minimal loss of maximum conductivity in the high temperature regime. Improved proton conductivity in the low temperature regime is necessary to facilitate fuel cell start-up at ambient temperatures.

The normalized plot of copolymer conductivity vs. $T-T_g$ (Fig. 5) clearly shows the effect of charge carrier reduction in

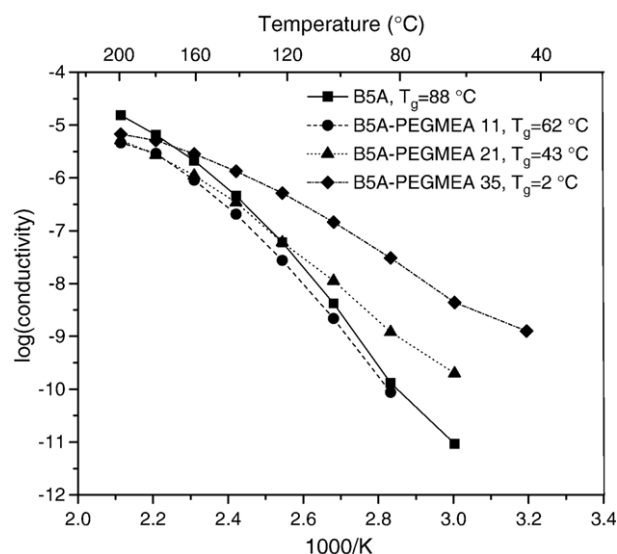


Fig. 4. Conductivity vs. temperature for B5A-PEGMEA copolymers.

the system. An initially large shift for B5A-PEGMEA 11 is seen followed by incremental shifts with increasing PEG incorporation. Weight percent of benzimidazole contained in each polymer is listed in Table 2, the weight percent is calculated by dividing the equivalent weight of the benzimidazole unit (117 g/mol) by the equivalent weight of the polymer repeat unit. In the case of the homopolymers this is the molecular weight of the monomer, whereas in the copolymers the equivalent weight of the repeat unit is defined as [(mol fraction B5A)(MW of B5A) + (mol fraction PEGMEA)(M_n of PEGMEA)]. It is interesting to note that at low PEG incorporation, the conductivity appears to be dominated by the reduction in charge carrier density, evidenced by the reduced conductivity of B5A-PEGMEA11 over B5A even though a reduction in T_g of 26 °C was achieved. However, as PEG incorporation increases the overall system mobility plays an increasingly dominant role such that the conductivity of B5A-PEGMEA35 is higher than B5A up to 160 °C despite a 35% reduction in benzimidazole content.

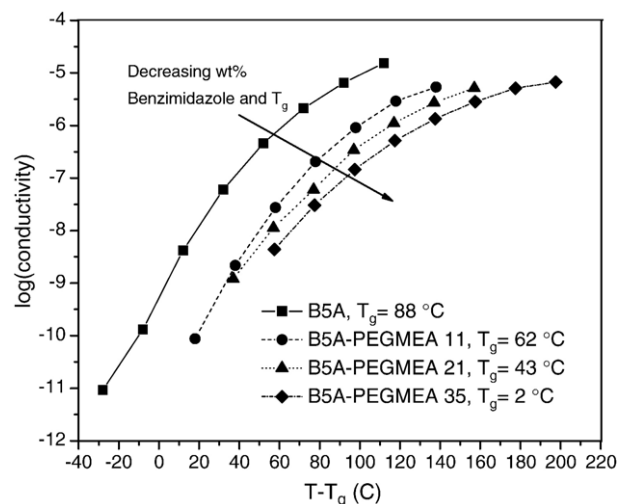
Fig. 5. Conductivity vs. $T-T_g$ for B5A-PEGMEA copolymers.

Table 3
Polymer structure-glass transition temperature comparison

Polymer	Structure	T_g , °C	Ref.
ABA tri-block PEG with benzimidazole tethered to the A blocks		~0	[22]
B5A-PEGMEA 35		2.0	This work
Polysiloxane copolymer with tethered benzimidazole (~32 mol%)		~50	[15]
Polystyrene-PEG comb-like polymers with tethered benzimidazole		57	[19]
Polystyrene with tethered imidazole		51	[19]

3.3. Structural effects

In cases where benzimidazole moieties are tethered to polymers to facilitate proton conduction there is a significant increase in T_g over the parent polymer regardless of the backbone type. While decreases in the polymer T_g by changing backbone type does result in increased conductivity values over the entire observed temperature range, there is an apparent lower T_g limit of approximately 50 °C (as observed in this and other work [15,24]), therefore, further T_g reduction must be accomplished through alternate polymer structural changes. Random siloxane copolymers containing tethered benzimidazole units display a steep rise in T_g as the mol% of benzimidazole is increased to 30% [15], while polystyrene-PEG comb-like polymers where the PEG side chains contain a benzimidazole unit on every repeat unit, result in significant

increases in T_g over the parent polymer [24]. Effective lowering of T_g through random copolymerization of B5A with PEGMEA demonstrates that tethered benzimidazole–benzimidazole interactions can be partly disrupted by introduction of PEG side chains randomly throughout the structure. The PEG ABA triblock copolymers with benzimidazole tethered to the A blocks prepared by Persson and Jannasch demonstrate similar T_g reduction effects [25]. Block copolymers containing 22 mol% benzimidazole display a T_g around 0 °C, consistent with our reported T_g of 2 °C at 23% benzimidazole. Comparison of polymer structures and their respective T_g values are listed in Table 3. The lower T_g observed upon disruption of benzimidazole interaction results in increased conductivity values in the low temperature regime due to increased segmental mobility with minimal impact on maximum conductivity values, increasing the useful temperature range of tethered benzimidazole materials. However, attention must be paid to the competing effect of charge carrier reduction on conductivity.

In addition to the polymer backbone type and comonomer choice, benzimidazole–benzimidazole interactions play a significant role in determining the polymer T_g . Alternatively, there is evidence that imidazole does not result in the same T_g increases over parent polymers observed for benzimidazole, polystyrene containing tethered imidazole shows a decrease in T_g over the parent polymer (Table 3), with the decrease dependent on the imidazole tether length [19]. Investigation into the effects of heterocycle choice on conductivity and polymer T_g is currently underway in our labs and will be the subject of future publications.

While we acknowledge that the polymers investigated in this work lack the long term stability for use as membranes in fuel cells due to chemical and thermal instabilities, the information gained will aid in optimization of charge carrier, backbone type, comonomer, and copolymer architecture. In future work, controlled polymerization of thermally and chemically stable monomers will produce well-defined copolymer structures and membranes designed to perform over a wide temperature range (40–200 °C).

4. Summary

Conductivity of polymers containing immobilized benzimidazole moieties was investigated as a function of polymer T_g . Decreases in T_g resulted in increases in conductivity, however, T_g was strongly influenced by intermolecular forces between benzimidazole units, resulting in T_g values higher than expected for the polymer architectures investigated. As observed in this work and elsewhere, this limits the operable temperature range of these types of anhydrous proton conducting systems. The prepared homopolymers reveal two competing trends, the effect of reduced T_g and the influence of charge carrier density on conductivity. Comparison of B5A and B5MA (46 wt.% and 43 wt.% benzimidazole respectively) demonstrates that reduction in T_g results in a significant increase in conductivity over the entire probed temperature range. However, when comparison of B5NB (36 wt.% benzimidazole) and B5MA is made, the effect of reduced T_g is offset by the difference in charge carrier density resulting in nearly identical conductivity vs. temperature curves.

Random copolymerization of the acrylate functional benzimidazole (B5A) monomer with poly(ethylene glycol) methyl ether acrylate ($M_n=454$ g/mol) resulted in decreased T_g over the parent homopolymer. The lower T_g results in increased conductivity at temperatures below 160 °C, broadening the potential useful range of these types of systems. However, convergence of the conductivity curves is observed as the temperature is increased reaching a maximum value ~ 0.5 orders of magnitude lower than B5A, consistent with a decrease in charge carrier density as the weight percent of benzimidazole is reduced. Therefore, to achieve significant increases in conductivity of heterocyclic systems over a broad temperature range, a balance of low T_g and high charge carrier density must be met through judicious choice of heterocycle, polymer backbone, and property modifying comonomers.

Acknowledgements

Funding provided by DOE EERE Subcontract #10759-001-05. Analytical facilities are made available through the NSF-supported Materials and Research Science and Engineering Center on Polymers at UMass Amherst (DMR-0213695). Mass spectral data were obtained at the University of Massachusetts Mass Spectrometry Facility which is supported, in part, by the National Science Foundation. The authors would like to thank MARKEM Corporation, Keene, NH for use of their Perkin Elmer Pyris 1 TGA, Brucker IFS 66v/S and related analytical facilities and Dr. Sergio Granados-Focil for valuable discussions.

References

- [1] EG & G Sevcics Parsons Incorporated, Fuel Cell Handbook, U.S. Department of Energy Office of Fossil Fuel Energy, 2000.

- [2] M. Zalbowitz, T., S., Fuel Cells: Green Power, U.S. Department of Energy, 1999.
- [3] L. Carrette, K.A. Friedrich, U. Stimming, Fuel Cells 1 (1) (2001) 5.
- [4] B.C.H. Steele, A. Heinzel, Nature 414 (2001) 345.
- [5] R.M. Rikukawa, K. Sanui, Prog. Polym. Sci. 25 (2000) 1463.
- [6] A.L. Rusanov, D.Y. Likhatchev, K. Mullen, Russ. Chem. Rev. 71 (9) (2002) 761.
- [7] A.M. Hickner, H. Ghassemi, Y.S. Kim, B.R. Einsla, J.E. McGrath, Chem. Rev. 104 (2004) 4587.
- [8] K.D. Kreuer, Solid State Ionics 94 (1–4) (1997) 55.
- [9] K.D. Kreuer, A. Fuchs, M. Ise, M. Spatch, J. Maier, Electrochim. Acta 43 (1998) 1281.
- [10] Q. Li, R. He, J.O. Jensen, N.J. Bjerrum, Chem. Mater. 15 (2003) 2896.
- [11] M. Schuster, W.H. Meyer, Annu. Rev. Mater. Res. 33 (2003) 233.
- [12] M. Schuster, T. Rager, A. Noda, K.D. Kreuer, J. Maier, Fuel Cells 5 (3) (2005) 355.
- [13] M.F.H. Schuster, W.H. Meyer, M. Schuster, K.D. Kreuer, Chem. Mater. 16 (2004) 329.
- [14] G.R. Goward, M.F.H. Schuster, D. Sebastiani, I. Schnell, H.W. Speiss, J. Phys. Chem., A 106 (2002) 9322.
- [15] C.J. Persson, P. Jannasch, Macromolecular 38 (2005) 3283.
- [16] R.C. Woudenberg, E.B. Coughlin, Tetr. Lett. 46 (2005) 6311.
- [17] J. Brandrup, E.H. Immergyt, E.A. Grulke, Polymer Handbook, 4th ed.; John Wiley & Sons, Inc., New York, 1999.
- [18] V. Galiatsatos, Polymer Data Handbook, Oxford University Press, New York, 1999, p. 698.
- [19] H.G. Herz, K.D. Kreuer, J. Maier, G. Scharfenberger, M.F.H. Schuster, W.H. Meyer, Electrochim. Acta 48 (2003) 2165.
- [20] K.-D. Kreuer, Chem. Mater. 8 (1996) 610.
- [21] M.F.H. Schuster, W.H. Meyer, Annu. Rev. Mater. Res. 33 (2003) 233.
- [22] M.A. Ratner, Polymer Electrolyte Reviews, Elsevier Applied Science, New York, 1987, p. 173.
- [23] As reported by Sartomer Company, I., 502 Thomas Jones Way, Exton, PA 19341, In.
- [24] C.J. Persson, P. Jannasch, Solid State Ionics 177 (2006) 653.
- [25] C.J. Persson, P. Jannasch, Chem. Mater. 18 (2006) 3096.